Article

Blinded study: prospectively defined high frequency oscillations predict seizure outcome in individual patients

DIMAKOPOULOS, Vasileios, *et al*.

Abstract

Interictal high frequency oscillations are discussed as biomarkers for epileptogenic brain tissue that should be resected in epilepsy surgery to achieve seizure freedom. The prospective classification of tissue sampled by individual electrode contacts remains a challenge. We have developed an automated, prospective definition of clinically relevant high frequency oscillations in intracranial EEG from Montreal and tested it in recordings from Zurich. We here validated the algorithm on intracranial EEG that was recorded in an independent epilepsy centre so that the analysis was blinded to seizure outcome. We selected consecutive patients who underwent resective epilepsy surgery in Geneva with postsurgical follow-up > 12 months. We analysed long-term recordings during sleep that we segmented into intervals of 5 minutes. High frequency oscillations were defined in the ripple (80-250 Hz) and the fast ripple (250-500 Hz) frequency bands. Contacts with the highest rate of ripples co-occurring with fast ripples designated the relevant area. As a validity criterion, we calculated the test-retest reliability of the high [...]

Reference

DIMAKOPOULOS, Vasileios, *et al*. Blinded study: prospectively defined high frequency oscillations predict seizure outcome in individual patients. *Brain Communications*, 2021

DOI : 10.1093/braincomms/fcab209
PMID : 34541534

Blinded study: prospectively defined high frequency oscillations predict seizure outcome in individual patients

Vasileios Dimakopoulos [1], Pierre Mégevand[2, 3], Ece Boran[1], Shahan Momjian[4], Margitta Seeck[3], Serge Vulliémoz[3], Johannes Sarnthein[1, 5*]

[1] Klinik für Neurochirurgie, UniversitätsSpital Zürich, Universität Zürich, Switzerland

[2] Département des neurosciences fondamentales, Faculté de médecine, Université de Genève, Switzerland

[3] Service de neurologie, Hôpitaux Universitaires de Genève, Switzerland

[4] Service de neurochirurgie, Hôpitaux Universitaires de Genève, Switzerland

[5] Klinisches Neurowissenschaften Zentrum, University Hospital Zurich, Switzerland

*** Correspondence:** johannes.sarnthein@usz.ch

UniversitätsSpital Zürich, Frauenklinikstrasse 10, 8091 Zürich, Switzerland

Short title: HFO predict postsurgical seizure freedom

Abstract

Interictal high frequency oscillations are discussed as biomarkers for epileptogenic brain tissue that should be resected in epilepsy surgery to achieve seizure freedom. The prospective classification of tissue sampled by individual electrode contacts remains a challenge. We have developed an automated, prospective definition of clinically relevant high frequency oscillations in intracranial EEG from Montreal and tested it in recordings from Zurich. We here validated the algorithm on intracranial EEG that was recorded in an independent epilepsy centre so that the analysis was blinded to seizure outcome.

We selected consecutive patients who underwent resective epilepsy surgery in Geneva with postsurgical follow-up > 12 months. We analysed long-term recordings during sleep that we segmented into intervals of 5 minutes. High frequency oscillations were defined in the ripple (80-250 Hz) and the fast ripple (250-500 Hz) frequency bands. Contacts with the highest rate of ripples co-occurring with fast ripples designated the relevant area. As a validity criterion, we calculated the test-retest reliability of the high frequency oscillations area between the 5 min intervals (dwell time ≥50%). If the area was not fully resected and the patient suffered from recurrent seizures, this was classified as a true positive prediction.

We included recordings from 16 patients (median age 32 years, range 18-53 years) with stereotactic depth electrodes and/or with subdural electrode grids (median follow-up 27 months, range 12-55 months). For each patient, we included several 5 min intervals (median 17 intervals). The relevant area had high test-retest reliability across intervals (median dwell time 95%). In two patients, the test-retest reliability was too low (dwell time < 50%) so that outcome prediction was not possible. The area was fully included in the resected volume in 2/4 patients who achieved postoperative seizure freedom (specificity 50%) and was not fully included in 9/10 patients with recurrent seizures (sensitivity 90%), leading to an accuracy of 79%. An additional exploratory analysis suggested that high frequency oscillations were associated with interictal epileptic discharges only in channels within the relevant area and not associated in channels outside the area.

We thereby validated the automated procedure to delineate the clinically relevant area in each individual patient of an independently recorded dataset and achieved the same good accuracy as in our previous studies. The reproducibility of our results across datasets is promising for a multicentre study to test the clinical application of high frequency oscillations to guide epilepsy surgery.

Keywords: Ripples, Fast ripples, automated detection, epilepsy surgery, intracranial EEG

Abbreviations

AEM	antiepileptic medication
CI	confidence interval
FN	false negative
FP	false positive
FR	fast ripple
FRandR	fast ripple co-occurring with ripple
HFO	high frequency oscillation
IED	interictal epileptic discharge
iEEG	intracranial EEG
ILAE	International League Against Epilepsy
NPV	negative predictive value
NREM	non rapid eye movement
PPV	positive predictive value
RV	resected brain volume
SNR	signal-to-noise ratio
SOZ	seizure onset zone
TN	true negative case
TP	true positive case

Introduction

Drug-resistant focal epilepsy is a common condition. In selected patients, surgical resection of the epileptogenic zone is the treatment of choice and may eliminate occurrence of seizures completely (1). The epileptogenic zone is defined as the minimum brain area whose resection leads to freedom from seizures (2). Preoperative diagnostic workup may involve recording of the intracranial EEG (iEEG) to determine the seizure onset zone (SOZ) as an estimate for the epileptogenic zone. Since seizures are usually rare events during the limited duration of the iEEG recording, it would be advantageous to determine the epileptogenic zone during the interictal period. In this approach, the traditional analysis of interictal epileptic discharges (IED) has a high sensitivity but low specificity as an interictal marker of epileptogenic tissue (3), which may be improved by more advanced analysis (4).

As a further marker, high frequency oscillations (HFO) may have the potential to be a clinical asset for delineating epileptogenic brain areas and identifying successful surgical treatments (3, 5-10). These oscillatory events can be found in the frequency range between 80–500 Hz. HFO are sub-classified in ripples (80-250 Hz) and fast-ripples (FRs, 250-500 Hz). Interictal HFO have proven to be more specific than interictal spikes in localizing the SOZ or 'predicting' seizure outcome (11-16). Many studies present HFO rates in relation to SOZ electrodes (17). Fewer studies analyse the resection of interictal HFO, marked prospectively, for the 'prediction' of post-surgical seizure freedom (7, 14, 15, 18-20).

Investigations in the clinical relevance of HFO have been facilitated by automated or semi-automated detection algorithms (20). Here we apply a fully automated definition of HFO, which we previously optimized on visual markings in a dataset of the Montreal Neurological Institute (21) and then validated on independently recorded data from Zurich (7). We thus provide a prospective definition of a clinically relevant HFO.

In the present study, we applied this algorithm to iEEG recorded in an independent epilepsy centre (Hôpitaux Universitaires de Genève, Switzerland). The analysis was blind with respect to clinical outcome. We compared the HFO area with the resected brain volume (RV) and 'predicted' the seizure outcome in individual patients in order to evaluate the clinical relevance of our algorithm for HFO analysis.

Materials and Methods

Patients

We included patients with drug-resistant focal epilepsy who 1) underwent invasive EEG recordings with subdural and/or depth electrodes as part of their presurgical evaluation in Geneva between 2015 and 2019, 2) underwent resective surgery and 3) were followed for at least one year after surgery. The decision for resective surgery was based on non-invasive investigations as well as on intracranial investigations (3). The results of the HFO analysis were not used for surgical planning. The postsurgical seizure outcome was determined by follow-up visits and classified according to the International League Against Epilepsy (ILAE).

Ethics statement

The study was approved by the research ethics committees (Cantonal ethics commissions of Zurich and of Geneva) and waived collection of patients' written informed consent 2019-01977). The study was performed in accordance with the relevant guidelines and regulations. As it is a blinded study, only the clinical information given in the tables was transferred from Geneva to Zurich. For the data transfer, the treating doctors in Geneva assigned a number to each patient. The researchers in Zurich used this number to match the results of the HFO analysis with clinical information. Patient confidentiality was maintained at all times.

Electrode types and implantation sites

Subdural grid electrodes as well as depth electrodes were placed according to the findings of the non-invasive presurgical evaluation. In 15 patients, depth electrodes (varying electrode configurations, AdTech, www.adtechmedical.com, and Dixi Medical, www.diximedical.com) were implanted stereotactically. In Patients 10 and 16, subdural grid and strip electrodes (contact diameter 4 mm with 2.3 mm exposure, spacing between contact centres 10 mm, AdTech) were placed after craniotomy. Pre-implantation MR and post-implantation CT images were used to locate each electrode contact anatomically using the intracranial electrode localization and visualization toolbox (iELVis, **Figure 1A**) (22).

Data preprocessing

For our analysis we selected data that were recorded during NREM sleep. An experienced neurologist (PM) visually selected periods of NREM sleep along the following criteria. 1) The data was recorded in the first part of the night between 11 pm and 3 am. 2) Widespread activity in the delta band was present in iEEG traces. 3) The iEEG showed sleep spindles in some patients. 4) Prolonged movement artefacts were absent in the EKG channel. For each patient, data from one night was available from the archive and this night was one of the first nights after electrode implantation.

The iEEG was recorded against a common subcutaneous reference placed close to the vertex and then transformed to bipolar channels. The data was resampled from 2048 Hz to 2000 Hz using the polyphaser anti-aliasing filter in Matlab. We then divided the data into 5-minute intervals for further analysis. We identified channels from sensorimotor and occipital brain regions using iELVis, because these are thought to exhibit large numbers of physiological HFO (23).

Prospective definition of HFO

HFO were defined prospectively by the automated detector that we had previously trained and validated to detect visually marked events in datasets from the Montreal Neurological Institute (21) and that was then validated in an independent dataset from Zurich (7). In this sense, the HFO detection algorithm was prospective. While the data analysis in the present study was retrospective, it was applied by researchers who were blind to the postoperative seizure outcome.

In brief, the detector incorporates information from both time and frequency domain and operates in two stages. In the first stage – baseline detection – the Stockwell transform identifies high entropy segments with low oscillatory activity. The values of the envelope of the signal at these high entropy segments define the baseline. The second stage – HFO detection – is conducted separately for ripples (band-pass 80–240 Hz, stopband 70 Hz and 250 Hz, FIR equiripple filter with stopband attenuation 60 dB) and FRs (band-pass 250–490 Hz, stopband 240 Hz and 500 Hz). Events with the envelope of the filtered signal exceeding the amplitude threshold for at least 20 ms/10 ms are labelled as ripples/FR **(Figure 1B, C)**. The algorithm then identifies FRs overlapping with a ripple, which we define as a third type of HFO: FR co-occurring with ripples (FRandR, **Figure 1D**). There is no manual rejection of events in this fully automated algorithm.

Definition of the HFO area by rate thresholding

In each recording interval and each patient, we computed the HFO rate by dividing the HFO count per channel by the duration of the epoch in minutes. We then analysed the spatial distribution of HFO rates across channels. For each electrode in one recording interval there is a rate threshold (95^{th} percentile of the HFO rate distribution) whether the electrode is included in the HFO area. The ensemble of those channels whose rates exceeded the rate threshold was defined as the HFO area **(Figure 2A)**.

Reliability of the spatial distribution of the HFO area

We then tested whether the HFO area was simply a product of chance. We excluded spurious channels by testing the spatial distribution of the HFO area against chance (scalar product, 97.5% threshold) as follows.

We selected each interval pair and computed the normalized scalar product of the spatial distribution of the HFO rates (**Figure 2B**). The scalar product is 1 for highly overlapping spatial distributions of HFO rate and lower otherwise. To test the magnitude of the true scalar product against chance, we constructed a distribution of scalar products by randomly permuting (N = 10000) the order of channels for each interval. The true value of the scalar product was considered statistically significant if it exceeded the 97.5% percentile of the distribution. We report the percentage of interval pairs where the scalar product was significant (**Table 1**, test-retest intervals). Finally, we quantified the test-retest reliability of the HFO area over the ensemble of recording intervals by counting the percentage of intervals that each channel spent in the HFO area (dwell time, **Figure 3**). The dwell time for each channel was calculated across intervals. If the median dwell time for the electrodes in the HFO area was less than 50%, we considered the analysis unreliable. This might be due to, for example, persistent artefacts in the EEG. Patients with median dwell time < 50% were excluded from further analysis.

Clinical validation of HFO against seizure outcome

Automated HFO detection and analysis were blind to clinical information. We evaluated whether the HFO area was included in the resected volume (RV) to quantify the predictive value of the HFO area with respect to seizure outcome. The electrode positions in the RV were determined from post-resection MR coregistered to pre-implantation MR scans (22). Electrodes landing on the border of the resection were deemed to be part of the RV. To stay consistent with earlier publications (6, 7, 24) we use the following classification system. We defined as true positive (TP) a patient where the HFO area was not fully located within the RV, i.e. at least one channel of the HFO area was not resected and the patient suffered from recurrent seizures (ILAE 2–6). We defined as false positive (FP) a patient where the HFO area was not fully located inside the RV but who achieved seizure freedom (ILAE 1). We defined as false negative (FN) a patient where the HFO area was fully located within the RV but who suffered from recurrent seizures. We defined as true negative (TN) a patient where the HFO area was fully located inside the RV and who became seizure free. The positive predictive value was calculated as PPV = TP/(TP + FP), negative predictive value as NPV = TN/(TN + FN), sensitivity = TP/(TP + FN), specificity = TN/(TN + FP), and accuracy = (TP + TN)/N.

Statistical analysis

We used the Wilcoxon rank-sum test to compare distributions. We compared percentages with the chi-square test. We estimated the 95% confidence intervals (CI) of proportions by the binomial method. All statistical analyses were performed in Matlab. Statistical significance was established at $p<0.05$.

Data and code availability

All data needed to evaluate the conclusions in the paper are present in the paper.
The code of the HFO detector is freely available at the repository
https://github.com/ZurichNCH/Automatic-High-Frequency-Oscillation-Detector.
The webpage https://hfozuri.ch/ indexes all available data and code.

Results

Patients and seizure outcome

We included 16 patients in the study that fulfilled the inclusion criteria (**Table 1**). Complete seizure freedom (ILAE 1) was achieved in 5 patients (seizure-free rate 31%), while 11 patients suffered from seizure recurrence (ILAE 2 – 6). Ten of 16 patients (63%) experienced significant reduction in their seizure burden (ILAE 1-3). In two patients, the test-retest reliability was too low (dwell time < 50%) to meet the validity criterion. In the remaining patient group (N = 14), the mean follow-up for good outcome (34 ± 12 mo) was longer than for poor outcome (26 ± 12 mo) but the difference between the two distributions were not significant (p = 0.22 Wilcoxon rank-sum test).

HFO detection and test-retest reliability of the HFO area

The HFO detection algorithm was applied to the recordings of all 16 patients. The number of intervals and the types of recording electrodes varied across patients (**Table 1**). Over the group of patients, we identified ripples (median amplitude 17.4 μVpp, interquartile range 9.8 μVpp) and FR (median amplitude 10.6 μVpp, interquartile range 3.7 μVpp). We used the co-occurrence of a ripple and a FR (FRandR) to determine the HFO area in each patient. The channels in sensorimotor and occipital brain regions were never in the HFO area (**Supplementary Table 1**). The example patient showed high test-retest reliability of the HFO area (**Figure 2 B**). Five channels were in the HFO area during all 14 intervals (dwell time 100 %, 14 * 5 min = 70 min), one channel was in the HFO area during 9/14 intervals (64%), one channel during 5 intervals (36%) etc. (**Figure 3**). The median dwell time across all patients was 95% (**Table 1**).

In Patients 15 and 16, the presence of HFO was masked by continuous artefacts in the iEEG. Recordings in these two patients were with subdural grid electrodes only. Visual inspection confirmed a large number of artifacts in these recordings, which caused spurious HFO detections. Consequently, the test-retest reliability of the HFO area was low (dwell time < 50%, **Table 1**) so that the HFO area could not be determined.

The HFO area predicted seizure outcome in individual patients

For each of the 14 patients, we evaluated whether the HFO area was fully or partly resected. The HFO area was fully resected in 2 patients who achieved seizure freedom (TN). The HFO area was not fully resected in 9 patients who did not achieve seizure freedom (TP). The HFO area was not fully resected in 2 patients who nevertheless achieved seizure freedom (FP). The HFO area was fully resected in one patient who did not achieve seizure freedom (FN).

From these values we obtain specificity = 50% CI [6.7 93%], sensitivity = 90% CI [55 99%], NPV = 67%, CI [9 99%], PPV = 89% CI [48 97%], and accuracy = 79% CI [49 95%]. The low specificity is related to the small number of correctly predicted seizure-free patients (TN = 2/4 patients with ILAE 1). The high sensitivity is explained by the high number of patients where the recurrence of seizures was correctly predicted (TP = 9/10 patients with ILAE > 2). Of the patients where recurrent seizures were correctly predicted (TP = 9), the HFO area was not fully resected in 4 patients (44%), and the HFO area was completely dissociated from the RV in 5 patients (56%) **(Supplementary Table 1)**. When compared to the SOZ, the HFO area matched the SOZ completely in 7/14 and partially in 2/14 patients **(Supplementary Table 1)**.

Both in our analysis and current surgical planning, the FN case may stem from the limited coverage of the implanted electrodes. The high sensitivity (90%) and PPV (89%) suggest that automated HFO detection might have contributed to improved surgical planning, since 9 of the 10 patients in whom the HFO area was not fully resected suffered from recurrent seizures.

Combining the Geneva cohort and the Zurich cohort

When combining the Geneva cohort of this study (N = 14) with the Zurich cohort (N = 20) (7) that were analysed with the same HFO detection algorithm, we obtained specificity = 88% CI [63 98%], NPV = 79% CI [54 93%], sensitivity = 76% CI [47 92%], PPV = 87% CI [57 98%], accuracy = 82% CI [64 93%]. The prediction accuracy for this combined cohort is associated with the surgical planning (seizure free rate 50% CI [33 67%], p = 0.001 chi-square test).

Characteristics of the clinically relevant HFO (FRandR)

To estimate the spatial extent of the FRandR, we counted the instances where a FRandR was detected simultaneously on two adjacent recording channels. In the 14 patients, the number of simultaneous FRandR counts was 2030 out of the total of 58618 counts, i.e. 57603 (98%) FRandR were detected on one channel only. This provides an upper limit for the spatial extent of FRandR in our recordings.

Finally, we investigated the relationship between the FRandR and IED. In a simple approach, we marked the center time of each FRandR and averaged the iEEG [-1.5 +1.5] s around the centre times of all FRandR, i.e. we generated a FRandR-triggered average. In a representative channel from the HFO area of Patient 6, the resulting average waveform resembles the shape of an IED (**Figure 4A**). The FRandR occurred at the rising flank of the IED. The centre time occurred at a random phase of the FRandR so that the averaged waveform does not show high frequency content.

To quantify whether the FRandR were associated with IED, we computed the signal-to-noise ratio (SNR) of the FRandR-triggered average where the period [-0.2 0.2] s captured the IED signal and the period [-1.5 -1.1] s captured the noise. Across all channels, the SNR revealed a bimodal distribution (**Figure 4B**). We separated the two modes by setting a threshold at SNR = 8 because 99.5% of all channels outside the HFO area had SNR < 8. We labelled channels with SNR > 8 as showing an association of the FRandR with IED. When computing the percentage of channels with SNR > 8, in 13/14 patients all channels (100%) of the HFO area showed an association of the FRandR with IED (**Table 1**). The only channels within an HFO area and SNR < 8 occurred in Patient 5 (seven red counts below the SNR threshold in **Figure 4B**). For channels within the HFO area, the median SNR = 19 was higher than for channels outside the HFO area (median SNR = 3, $p < 0.0001$, Wilcoxon rank sum test). Also on the patient level, the SNR was higher within the HFO area than outside in 14/14 patients (**Supplementary Table 1**, $p < 0.001$ paired Wilcoxon sign rank test). On the channel level, the FRandR were associated with the IED only in channels within the HFO area but not in channels outside the HFO area ($p < 0.000001$ chi-square test).

Discussion

In the current study, we have applied an automated definition of clinically relevant HFO on an independently recorded dataset and 'predicted' postoperative seizure recurrence or seizure freedom with good accuracy. While the data analysis was retrospective, the HFO detection algorithm had been defined prospectively and was applied by researchers who were blind to postoperative seizure outcome. As an integral part of the algorithm, the test-retest analysis of the HFO area proved the outcome prediction to be valid in 14 of the 16 patients. We have thereby further validated our definition of a clinically relevant HFO.

Reliability of HFO as markers of the epileptogenic zone

The delineation and the clinical evaluation of the HFO area provided high sensitivity (90%) in predicting seizure recurrence: if the HFO area was not fully resected, then seizure freedom (ILAE 1) was not achieved. The high sensitivity could be associated with the capability of the HFO to generalize across individual patients. Contrary to a previous multicentre study (25), we were able to accurately correlate the seizure outcome with the HFO area. This discrepancy might be explained by the definition of a clinically relevant HFO; based on our previous study, we define the co-occurrence of ripples and fast ripples (FRandR) as biomarker for the epileptogenic zone because FRandR have been proven more specific than ripples or fast ripples (7).

In our previous study (7), the high specificity of FRandR rendered a false positive (FP) classification unlikely, which in turn would prevent patients from receiving a larger resection than necessary. This previous finding (7) could not be corroborated here (Tables 1, 2) because of the small number of patients that achieved seizure freedom. Therefore, the algorithm needs to be tested further on large datasets with artefact-free recordings to reduce the width of the confidence intervals even more than what could be achieved by combining the Geneva and the Zurich cohort.

The detection of HFO can be challenging because of their low signal-to-noise ratio and artefacts in the iEEG. In meeting this challenge, our HFO detector was designed for HFO detection during NREM sleep (7, 21). The automated analysis pipeline results in a prospective definition of the HFO area. Distinct from other studies that consider only visual markings, we use here the test-retest reliability of the spatial distribution of the HFO (dwell time). The reproducibility of the HFO area across the data intervals can be explained by the high internal consistency of the HFO rates across the intervals. It supports HFO as reliable biomarker for epileptogenic brain tissue.

In two patients (15 and 16), the test-retest reliability was low (dwell time < 50%). These patients did not differ in outcome from the rest of the patient group. Possibly, the recording with subdural as opposed to depth electrodes may sometimes result in artefact-loaded data which may render HFO detection impossible. Interestingly, these patients are examples where the test-retest approach helped to make the HFO analysis pipeline more reliable.

There were HFO both inside and outside of the HFO area in our data. This may have several reasons:
1) Epilepsy is a network disease and HFO appear at distributed locations of the network.
2) The limited time of iEEG recording during a few days may point to an HFO area that might not reflect the epileptogenic zone. Our prospective definition of HFO was validated against the resection of the epileptogenic zone.
3) Our prospective definition of a clinically relevant HFO focuses on the co-occurrence of a ripple and a fast ripple (FRandR). It thereby ignores the traditional distinction between ripples (80-250 Hz) and FR (250-500 Hz) (26). While the rate of FRandR is obviously lower than the rates of ripples and FR separately, this definition may still be highly sensitive but not ultimately specific, e.g. events might be labelled as epileptic FRandR, which in fact they are not. In view of these considerations, we had introduced the 95% rate threshold to label a channel as member of the HFO area and the consistency of this labelling over time (dwell time) to gauge the reliability of the HFO area (7).

Finally, it is being debated whether HFO may show variability in their location over prolonged recordings (7, 27-29). A large study reported that HFO rates vary widely over time (27). A recent study (28) investigated high frequency activity (80-170 Hz) over several weeks and found that its spatiotemporal profile did not reflect the long term behaviour after the electrode implantation. The high variability found in these two studies (27, 28) is at variance with the high stability found with our algorithm. While the recording intervals in the present study were all from the same night of a patient, our earlier application of the algorithm has revealed a high test-retest reliability of FRandR rates over several nights (7). We use the test-retest reliability as a criterion for the applicability of FRandR analysis, which is supported by the respectable accuracy of 82% in prediction of seizure outcome in the combined Geneva-Zurich cohort. This accuracy is only obtained for FRandR (7), i.e. short events with appreciable energy in the whole frequency range 80-500 Hz, and not for Ripples (80-250 Hz). The FRandR are very different from the HFO defined by Gliske et al. (27) and the high frequency activity (80-170 Hz) that was called into question by Chen et al. (28). Obviously, our blinded study approach should be extended to more and larger patient cohorts (29). Furthermore, analysis of iEEG recordings would be highly desirable over longer time periods, which might be facilitated by a low power device that is dedicated to FRandR detection (30).

Let us now recall the key points of our algorithm. First, we investigate FRandR (80-500 Hz), i.e. short events with appreciable energy up to 500 Hz. This is very different from high frequency activity (80-170 Hz) as investigated in (28). Second, we are very careful in including only periods of NREM sleep (8). Third, we use an automated detector that has been validated against seizure outcome in a large dataset (21). This algorithm has achieved high test-retest reliability of the spatiotemporal FRandR profile in the majority of patients during the time of recording. The good accuracy in predicting postoperative seizure outcome indicates that FRandR as markers of the epileptogenic zone are stable over time.

Electrophysiological characteristics of FRandR

Regarding their spatial spread, the vast majority of FRandR (98%) was detected on one channel only. This is in agreement with an earlier report that detected FR usually in just one channel (31) and in line with general considerations that electrophysiological features with higher frequencies tend to have smaller spatial extent (32).

How are FRandR related to IED? In 13/14 patients, all channels within the HFO area – but not outside - showed a FRandR-triggered average with high SNR (**Figure 4, Table 1**). This suggests that a FRandR is commonly associated with the occurrence of an IED. Certainly, several FRandR occurred without an IED but these were overruled in the average and, conversely, several IED occurred without FRandR. In scalp EEG, IED associated with HFO are more specific to epileptic tissue than the general population of IED (33). Analogously, we hypothesize that the FRandR detected by our algorithm are associated with IED, and that

this association may be a biomarker for pathological activity by which the underlying epileptogenic tissue might be delineated in future studies.

Seizure outcome

In our cohort, the rate of post-operative seizure freedom was relatively low (31%), although a majority of patients (63%) experienced a significant reduction in their seizure burden. In our opinion, this reflects the clinical practice of the study centre, where iEEG implantation is reserved to the most complex cases. Our case mix contains a high proportion of patients with long-standing, non-lesional extratemporal lobe epilepsy, who have a poorer prognosis for postoperative seizure freedom (34, 35). In fact, our outcomes do not differ significantly from those in a large cohort of non-lesional extratemporal lobe epilepsy (36).

Even though the follow-up of seizure-free patients exceeds 18 months, seizure freedom might not persist in the future. Out of five patients with outcome ILAE 1, four are still taking antiepileptic medication (AEM). The majority of data on stopping AEM after successful epilepsy surgery come from anterior temporal lobe resection series. In our case mix, we tend to err on the side of caution and leave AEM for at least a full 2 years, sometimes more, depending on each patient's expectations (e.g. if continued fitness to drive is more important to the patient than the complete withdrawal of AEM).

Clinical relevance and generalizability

In order for HFO analysis to obtain clinical relevance, HFO must be validated against seizure outcome, should be defined prospectively, and should be tested on sufficient data (8). The results of our algorithm suggest that the information provided by prospectively defined HFO could contribute to surgery planning in patients where the extent of surgical resection is difficult to define and can be adapted. It is in these patients where complementary electrophysiological markers such as HFO may be useful (5, 15, 29, 37). Different from IED, HFO do not propagate, which is an advantage if the epileptic zone needs to be localized precisely (9, 16). A growing number of studies relates the presence of HFO to surgical outcome (20, 38). A prospective, automated definition of HFO renders HFO analysis more generalizable (7, 18, 19). Further, the algorithm used here was previously trained and validated on datasets from two epilepsy centres (7, 21). These HFO markings served as benchmark for a device that detects HFO in real time (30). The good performance of the detector on an independent third dataset supports the generalizability and clinical relevance of HFO analysis.

Conclusions

In a blinded study design, we validated the automated procedure to delineate the clinical relevant HFO area in individual patients of an independently recorded dataset. The HFO were associated with IED in the HFO area. HFO analysis showed a very good sensitivity and PPV, i.e. if HFO remained outside the resection volume, it was more likely that the patient continued to seize. Together with an intermediate specificity and NPV, this achieved the same good accuracy as in our previous studies. The reproducibility of our results across datasets is promising for a multicentre study testing the clinical application of HFO detection to guide epilepsy surgery.

Funding

We acknowledge grants awarded by the Swiss National Science Foundation (SNSF 176222 to JS, SNSF 192749 to SV) and a SNSF Ambizione fellowship (PZ00P3_167836 to PM). The collaboration between the members of Université de Genève and Universität Zürich benefitted from joint seed money funding. The funders had no role in the design or analysis of the study.

Competing Interests

The authors declare that the research was conducted in the absence of any commercial or financial relationships that could be construed as a potential conflict of interest.

References

1. Ryvlin P, Rheims S. Predicting epilepsy surgery outcome. Curr Opin Neurol. 2016;29(2):182-8.
2. Rosenow F, Luders H. Presurgical evaluation of epilepsy. Brain : a journal of neurology. 2001;124(Pt 9):1683-700.
3. Jobst BC, Bartolomei F, Diehl B, Frauscher B, Kahane P, Minotti L, et al. Intracranial EEG in the 21st Century. Epilepsy Curr. 2020;20(4):180-8.
4. Megevand P, Spinelli L, Genetti M, Brodbeck V, Momjian S, Schaller K, et al. Electric source imaging of interictal activity accurately localises the seizure onset zone. J Neurol Neurosurg Psychiatry. 2014;85(1):38-43.
5. van 't Klooster MA, van Klink NEC, Zweiphenning W, Leijten FSS, Zelmann R, Ferrier CH, et al. Tailoring epilepsy surgery with fast ripples in the intraoperative electrocorticogram. Annals of neurology. 2017;81(5):664-76.
6. Fedele T, van 't Klooster M, Burnos S, Zweiphenning W, van Klink N, Leijten F, et al. Automatic detection of high frequency oscillations during epilepsy surgery predicts seizure outcome. Clinical neurophysiology : official journal of the International Federation of Clinical Neurophysiology. 2016;127(9):3066-74.
7. Fedele T, Burnos S, Boran E, Krayenbuhl N, Hilfiker P, Grunwald T, et al. Resection of high frequency oscillations predicts seizure outcome in the individual patient. Sci Rep. 2017;7(1):13836.
8. Fedele T, Ramantani G, Sarnthein J. High frequency oscillations as markers of epileptogenic tissue - End of the party? Clinical neurophysiology : official journal of the International Federation of Clinical Neurophysiology. 2019;130(5):624-6.
9. Jacobs J, Zijlmans M. HFO to Measure Seizure Propensity and Improve Prognostication in Patients With Epilepsy. Epilepsy Curr. 2020:1535759720957308.
10. Boran E, Sarnthein J, Krayenbuhl N, Ramantani G, Fedele T. High-frequency oscillations in scalp EEG mirror seizure frequency in pediatric focal epilepsy. Sci Rep. 2019;9(1):16560.
11. Liu S, Quach MM, Curry DJ, Ummat M, Seto E, Ince NF. High-frequency oscillations detected in ECoG recordings correlate with cavernous malformation and seizure-free outcome in a child with focal epilepsy: A case report. Epilepsia Open. 2017;2(2):267-72.
12. Akiyama T, McCoy B, Go CY, Ochi A, Elliott IM, Akiyama M, et al. Focal resection of fast ripples on extraoperative intracranial EEG improves seizure outcome in pediatric epilepsy. Epilepsia. 2011;52(10):1802-11.
13. Jacobs J, Zijlmans M, Zelmann R, Chatillon CE, Hall J, Olivier A, et al. High-frequency electroencephalographic oscillations correlate with outcome of epilepsy surgery. Annals of neurology. 2010;67(2):209-20.
14. Sumsky SL, Santaniello S. Decision Support System for Seizure Onset Zone Localization Based on Channel Ranking and High-Frequency EEG Activity. IEEE J Biomed Health Inform. 2019;23(4):1535-45.
15. Cuello-Oderiz C, von Ellenrieder N, Sankhe R, Olivier A, Hall J, Dubeau F, et al. Value of ictal and interictal epileptiform discharges and high frequency oscillations for delineating the epileptogenic zone in patients with focal cortical dysplasia. Clinical neurophysiology : official journal of the International Federation of Clinical Neurophysiology. 2018;129(6):1311-9.
16. Schonberger J, Huber C, Lachner-Piza D, Klotz KA, Dumpelmann M, Schulze-Bonhage A, et al. Interictal Fast Ripples Are Associated With the Seizure-Generating Lesion in Patients With Dual Pathology. Front Neurol. 2020;11:573975.
17. Cimbalnik J, Kucewicz MT, Worrell G. Interictal high-frequency oscillations in focal human epilepsy. Curr Opin Neurol. 2016;29(2):175-81.
18. Weiss SA, Berry B, Chervoneva I, Waldman Z, Guba J, Bower M, et al. Visually validated semi-automatic high-frequency oscillation detection aides the delineation of epileptogenic regions during intra-operative electrocorticography. Clinical neurophysiology : official journal of the International Federation of Clinical Neurophysiology. 2018;129(10):2089-98.

19. Nariai H, Hussain SA, Bernardo D, Fallah A, Murata KK, Nguyen JC, et al. Prospective observational study: Fast ripple localization delineates the epileptogenic zone. Clinical neurophysiology : official journal of the International Federation of Clinical Neurophysiology. 2019;130(11):2144-52.
20. Remakanthakurup Sindhu K, Staba R, Lopour BA. Trends in the use of automated algorithms for the detection of high-frequency oscillations associated with human epilepsy. Epilepsia. 2020;61(8):1553-69.
21. Burnos S, Frauscher B, Zelmann R, Haegelen C, Sarnthein J, Gotman J. The morphology of high frequency oscillations (HFO) does not improve delineating the epileptogenic zone. Clinical neurophysiology : official journal of the International Federation of Clinical Neurophysiology. 2016;127(4):2140-8.
22. Groppe DM, Bickel S, Dykstra AR, Wang X, Megevand P, Mercier MR, et al. iELVis: An open source MATLAB toolbox for localizing and visualizing human intracranial electrode data. J Neurosci Methods. 2017;281:40-8.
23. Frauscher B, von Ellenrieder N, Zelmann R, Rogers C, Nguyen DK, Kahane P, et al. High-Frequency Oscillations in the Normal Human Brain. Annals of neurology. 2018;84(3):374-85.
24. van 't Klooster MA, van Klink NE, Leijten FS, Zelmann R, Gebbink TA, Gosselaar PH, et al. Residual fast ripples in the intraoperative corticogram predict epilepsy surgery outcome. Neurology. 2015;85(2):120-8.
25. Jacobs J, Wu JY, Perucca P, Zelmann R, Mader M, Dubeau F, et al. Removing high-frequency oscillations: A prospective multicenter study on seizure outcome. Neurology. 2018;91(11):e1040-e52.
26. Levesque M, Wang S, Gotman J, Avoli M. High frequency oscillations in epileptic rodents: Are we doing it right? J Neurosci Methods. 2018;299:16-21.
27. Gliske SV, Irwin ZT, Chestek C, Hegeman GL, Brinkmann B, Sagher O, et al. Variability in the location of high frequency oscillations during prolonged intracranial EEG recordings. Nature Communications. 2018;9(1):2155.
28. Chen Z, Grayden DB, Burkitt AN, Seneviratne U, D'Souza WJ, French C, et al. Spatiotemporal Patterns of High-Frequency Activity (80–170 Hz) in Long-Term Intracranial EEG. Neurology. 2021;96(7):e1070-e81.
29. Chen Z, Maturana MI, Burkitt AN, Cook MJ, Grayden DB. High-Frequency Oscillations in Epilepsy: What Have We Learned and What Needs to be Addressed. Neurology. 2021;96(9):439-48.
30. Sharifshazileh M, Burelo K, Sarnthein J, Indiveri G. An electronic neuromorphic system for real-time detection of high frequency oscillations (HFO) in intracranial EEG. Nature Communications. 2021;12(1):3095.
31. von Ellenrieder N, Dubeau F, Gotman J, Frauscher B. Physiological and pathological high-frequency oscillations have distinct sleep-homeostatic properties. Neuroimage Clin. 2017;14:566-73.
32. von Stein A, Sarnthein J. Different frequencies for different scales of cortical integration: from local gamma to long range alpha/theta synchronization. Int J Psychophysiol. 2000;38(3):301-13.
33. Cai Z, Sohrabpour A, Jiang H, Ye S, Joseph B, Brinkmann BH, et al. Noninvasive high-frequency oscillations riding spikes delineates epileptogenic sources. Proceedings of the National Academy of Sciences of the United States of America. 2021;118(17):e2011130118.
34. Garcia Gracia C, Yardi R, Kattan MW, Nair D, Gupta A, Najm I, et al. Seizure freedom score: A new simple method to predict success of epilepsy surgery. Epilepsia. 2015;56(3):359-65.
35. Jehi L, Yardi R, Chagin K, Tassi L, Russo GL, Worrell G, et al. Development and validation of nomograms to provide individualised predictions of seizure outcomes after epilepsy surgery: a retrospective analysis. Lancet Neurol. 2015;14(3):283-90.
36. Noe K, Sulc V, Wong-Kisiel L, Wirrell E, Van Gompel JJ, Wetjen N, et al. Long-term outcomes after nonlesional extratemporal lobe epilepsy surgery. JAMA Neurol. 2013;70(8):1003-8.
37. Wu JY, Sankar R, Lerner JT, Matsumoto JH, Vinters HV, Mathern GW. Removing interictal fast ripples on electrocorticography linked with seizure freedom in children. Neurology. 2010;75(19):1686-94.
38. Frauscher B. Localizing the epileptogenic zone. Curr Opin Neurol. 2020;33(2):198-206.

Figure legends

Figure 1: Automated HFO analysis in Patient 11

(A) Locations of the iEEG depth electrodes.

(B, C, D) HFO detection: example of a ripple co-occurring with an FR (FRandR). (B) Wideband iEEG (C) iEEG filtered in the ripple band [80 250] Hz (D) iEEG filtered in the fast ripple band [250 500] Hz. The HFO detection is highly specific: while several ripples and FRs were detected, only one FRandR was selected as a clinically relevant HFO. Ripple (R) blue; Fast ripple (FR) cyan; FRandR red; AD amygdala right; HAD hippocampus anterior right; HPD hippocampus posterior right.

Figure 2: HFO rate distribution for Patient 11

(A) HFO rate (FRandR, co-occurring ripple and fast ripple, HFO/min) for each interval (red vertical bar). Channels with rates that exceed the 95th percentile (black line) are candidates to be included in the HFO area (rate thresholding).

(B) The anatomical distribution of HFO is not random. The true distribution of the normalized scalar product of HFO rates for each pair of intervals (red). The random distribution of the normalized scalar product of HFO rates obtained by permutation analysis (grey, 10000 permutations). The 97.5th percentile of the random permutation (vertical blue line) serves as the significance threshold. 100% of the true distribution exceed the significance threshold; therefore the anatomical distribution of HFO is not random. AD amygdala right; HAD hippocampus anterior right; HPD hippocampus posterior right.

Figure 3: Test-Retest analysis of HFO rates for Patient 11

Reproducibility of the HFO area over recording intervals. Red bars denote channels where the HFO rate exceeds the 95th percentile in that interval. Channels from the tip of recording electrodes AD, HAD and HPD have red bars for a dwell time = 100% of the recording intervals. The last column illustrates the channels that meet the 95% criterion. The second but last column guides the eye.
AD amygdala right; HAD hippocampus anterior right; HPD hippocampus posterior right.

Figure 4: The FRandR-triggered average and its SNR distribution.

(A) To create this plot, we marked the centre time of each FRandR in a representative recording channel in the HFO area of Patient 6. We then averaged the iEEG [-1.5 +1.5] s around the centre times of all FRandR. The resulting average waveform resembles the shape of an interictal epileptic discharge (IED). The FRandR (t = 0 s) occurred at the rising flank of the IED. The centre time occurred at a random phase of the HFO so that the averaged waveform does not show high frequency content. We computed the signal-to-noise ratio (SNR= 24) of the FRandR-triggered average where the period [-0.2 0.2] s (black bar) captured the IED signal and the period [-1.5 -1.1] s (gray bar) captured the noise.

(B) The SNR distribution of the FRandR-triggered average is bimodal. We separate the two modes by a threshold at SNR = 8 (black dashed line). In channels with SNR > 8, we consider FRandR to be associated with IED. All the seven channels within the HFO area with SNR < 8 were recorded in Patient 5. For channels within the HFO area (red), the median SNR = 19 was higher than for channels outside the HFO area (gray, median SNR = 3, $p < 0.0001$, Wilcoxon rank sum test).

Tables

Table 1. Patient Characteristics

Postoperative seizure recurrence (ILAE > 1) was correctly 'predicted' in 11/14 patients. In two patients, 'prediction' was not possible.
The FRandR were associated with interictal epileptic discharges (i.e. SNR > 8) in all channels (100%) within the HFO area in 13/14 patients and in < 7% channels outside the HFO area in all patients.
Abbreviations: HS hippocampal sclerosis; FCD focal cortical dysplasia; WM white matter; ILAE International League Against Epilepsy; TP True Positive; TN True Negative; FP False Positive; FN False Negative; SNR Signal-to-Noise Ratio.

Patient	Sex	Histology	Electrode type	Bipolar channels	Intervals	Test-retest intervals (%)	Median dwell time (%)	Outcome (ILAE scale)	Follow-up (months)	Prediction ILAE >1	Channels within HFO area with SNR>8 (%)	Channels outside HFO area with SNR>8 (%)
1	F	No HS, no dysplasia	depth	42	25	100	89	1	48	TN	100	4
2	F	No abnormality	depth	70	21	63	74	1	34	TN	100	2
3	F	FCD type IIb	depth	70	10	90	83	1	36	FP	100	3
4	M	HS, WM ectopic neurons	depth	177	10	95	100	1	18	FP	100	1
5	F	Hippocampal gliosis	depth	76	17	84	75	4	32	TP	21	2
6	M	WM ectopic neurons	depth	77	8	100	100	5	12	TP	100	4
7	F	Cortical gliosis	subdural	81	13	88	79	4	18	TP	100	6
8	M	WM ectopic neurons	depth, subdural	82	21	80	94	3	30	TP	100	6
9	F	WM ectopic neurons	depth	123	14	96	89	3	55	TP	100	4
10	M	FCD type IIa	depth	126	18	100	89	4	24	TP	100	1

11	F	WM ectopic neurons	depth	129	14	100	100	3	21	TP	100	3
12	M	HS	depth	162	22	98	88	3	21	TP	100	1
13	M	WM ectopic neurons	depth	197	13	100	100	4	18	TP	100	2
14	M	No HS, no dysplasia	depth	106	16	98	100	5	30	FN	100	6
15	M	No dysplasia	subdural	74	19	43	45	1	16	--	--	--
16	F	WM ectopic neurons	subdural	112	16	52	46	3	45	--	--	--

Table 2. HFO area and seizure freedom

Resection of the HFO area has intermediate specificity in predicting the seizure freedom and is highly sensitive in predicting seizure recurrence. Abbreviations: TP = True Positive; TN = True Negative; FP = False Positive; FN = False Negative; N = number of patients; PPV = Positive Predictive Value; NPV = Negative Predictive Value;

Sensitivity	TP/(TP + FN)	90%
Specificity	TN/(TN + FP)	50%
Positive Predictive Value PPV	TP/(TP + FP)	82%
Negative Predictive Value NPV	TN/(TN + FN)	67%
Accuracy	(TP + TN)/N	79%

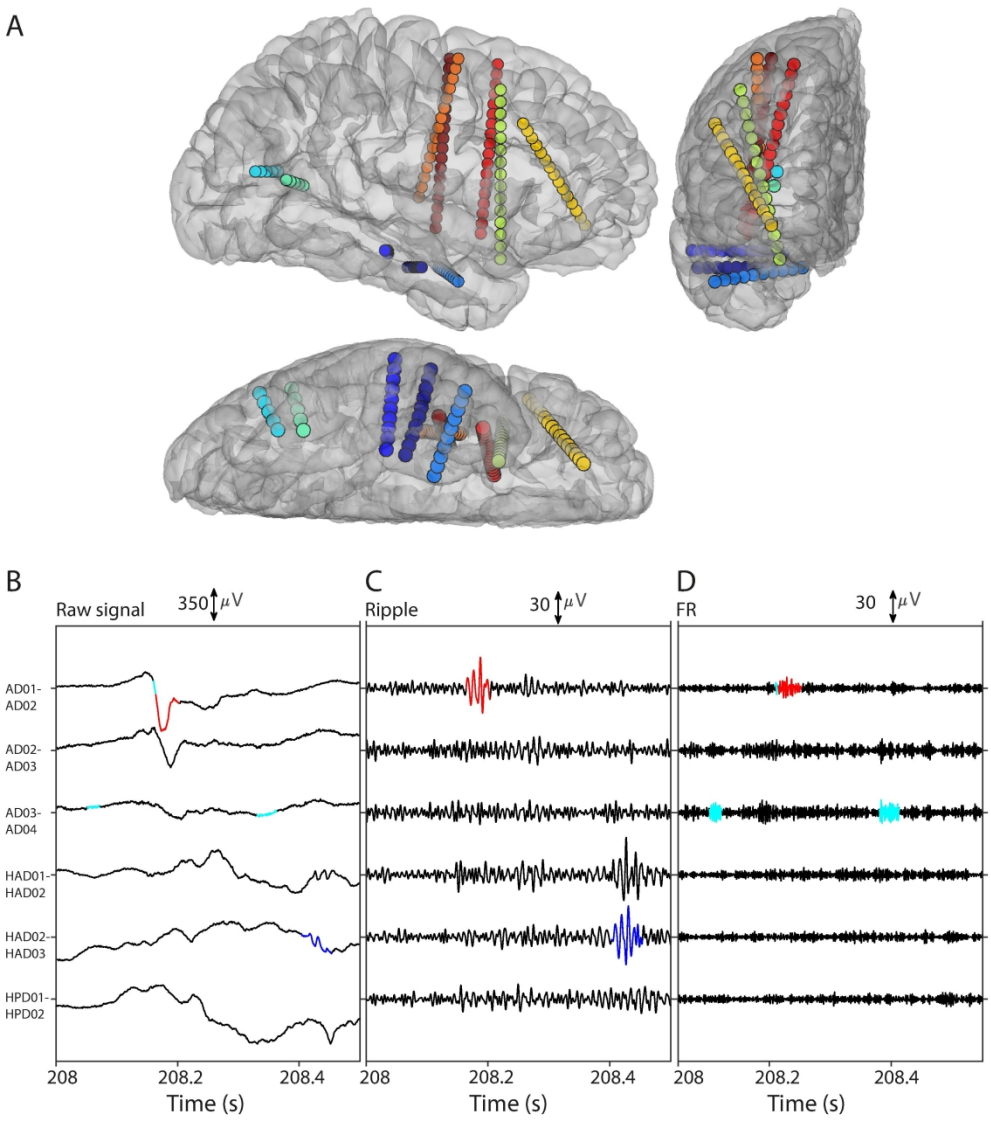

Figure 1

143x160mm (600 x 600 DPI)

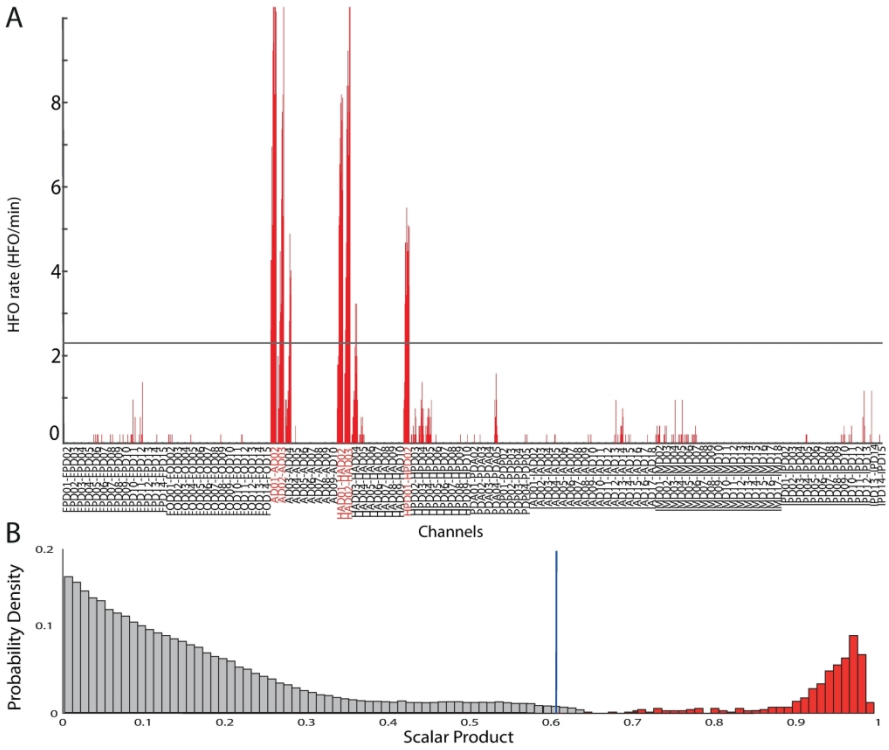

220x163mm (300 x 300 DPI)

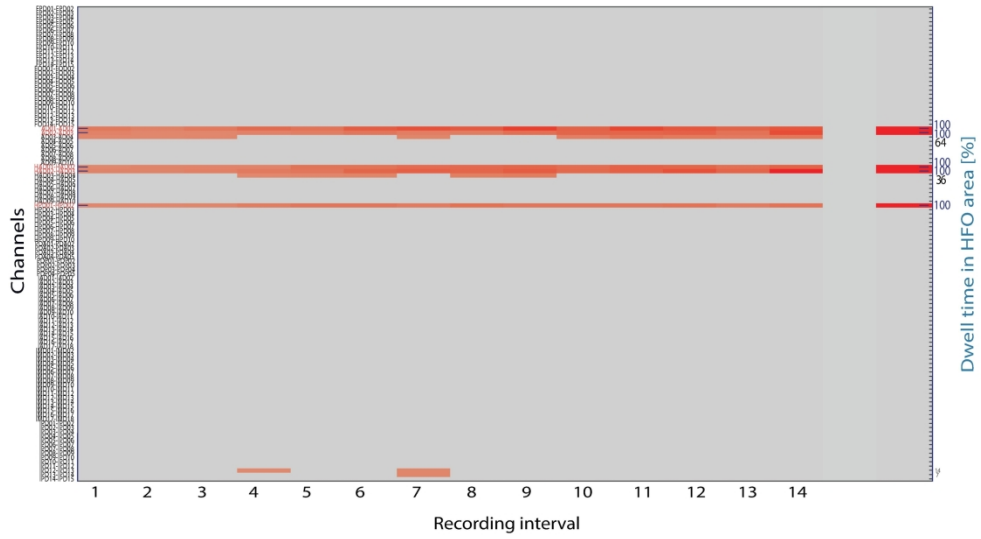

215x125mm (300 x 300 DPI)

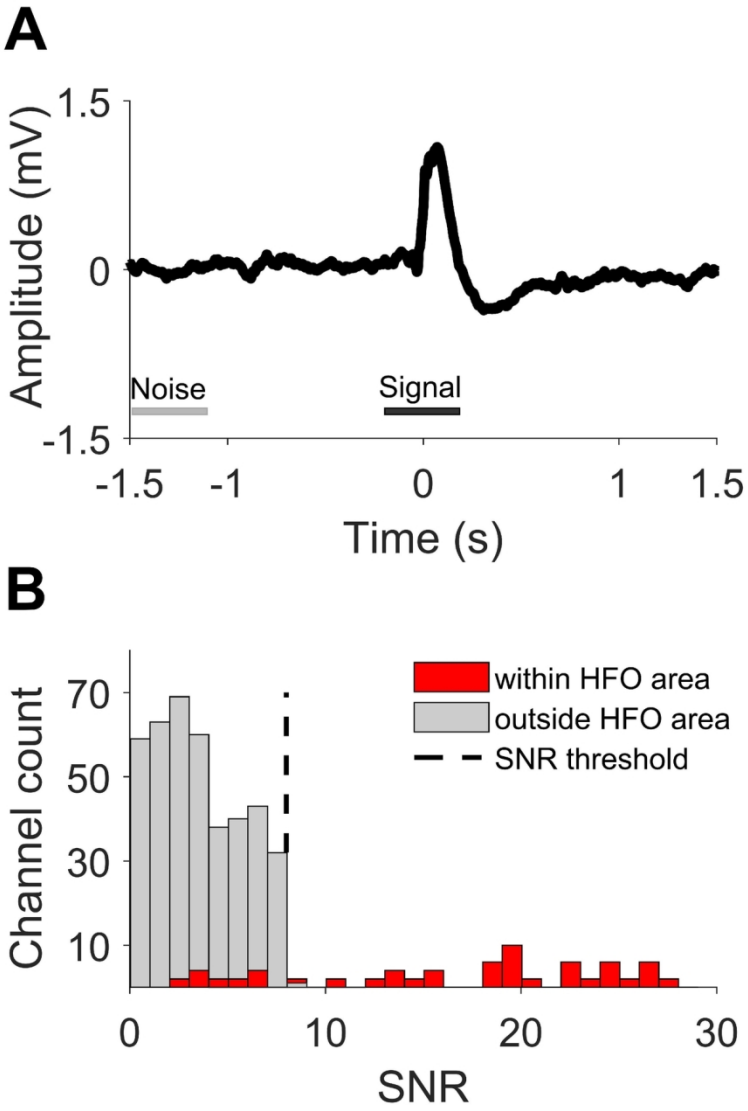

107x169mm (300 x 300 DPI)

Dimakopoulos et al. applied a fully automated HFO detection algorithm on presurgical iEEG recordings from patients that underwent resective epilepsy surgery. The analysis was blind to clinical outcome and achieved good ‘prediction’ of seizure outcome. The HFO reproducibility indicates the value of a future multicenter study to test clinical application.

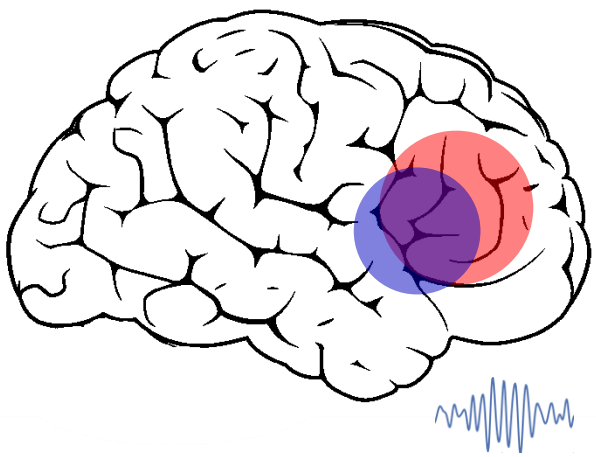

Area of high frequency oscillations
is not entirely resected

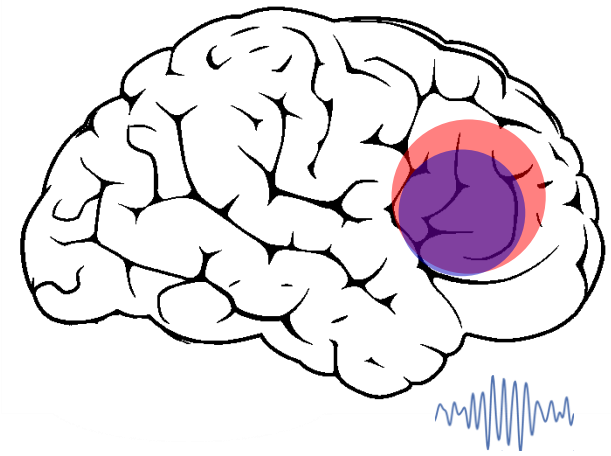

Area of high frequency oscillations
is entirely resected

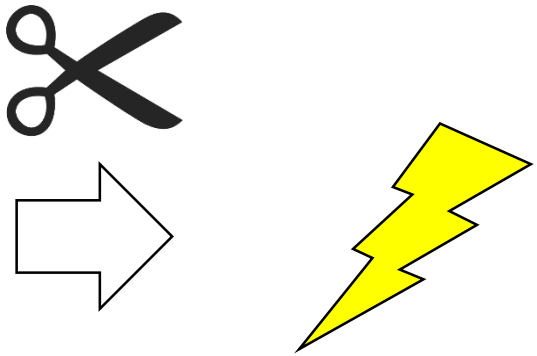

Seizure
recurrence

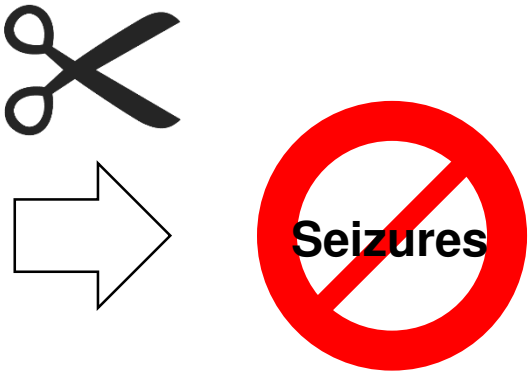

Seizure
freedom